Vol. 70: 39–55, 2016
doi: 10.3354/cr01416

CLIMATE RESEARCH
Clim Res

Published September 26

Diurnal cycle of precipitation simulated by RegCM4 over South America: present and future scenarios

Michelle Simões Reboita[1,*], Lívia Márcia Mosso Dutra[2], Cássia Gabriele Dias[1]

[1]Natural Resources Institute, Federal University of Itajubá, Av. BPS, 1303, Itajubá, Minas Gerais, MG 37500-903, Brazil
[2]Department of Atmospheric Sciences, University of São Paulo, Rua do Matão, 1226, Cid. Universitária, São Paulo, SP 05508-090, Brazil

ABSTRACT: The diurnal cycle of precipitation (DCP) is not the same in every region of the globe because it depends on the local dynamics and thermodynamics of each region. The main purpose of this study was to analyze the DCP simulated by the Regional Climate Model version 4 (RegCM4) nested in the HadGEM2-ES over South America in 3 time slices: historical (1998–2005), near (2020–2048), and far (2070–2098) future climates considering the austral summer and winter seasons. This work is part of the Phase I CORDEX RegCM4 hyper-Matrix (or CREMA) experiment and uses the RCP8.5 scenario for the future climate periods. The historical period is validated by comparing the simulation with the Tropical Rainfall Measuring Mission (TRMM-2A25 and TRMM-3B42 v7) and Global Satellite Mapping of Precipitation (GSMaP MVK+) datasets. The contrasts in the DCP between tropics and extratropics registered in TRMM and GSMaP are in general simulated by RegCM4. During summer, the model simulates the peak of precipitation at 18:00 UTC in the tropical and subtropical subdomains as in the satellite products. In winter, RegCM4 overestimates the precipitation in all subtropical subdomains, and the DCP is better simulated in the tropical region. Among the results for the future scenarios, in general, in summer the near future shows the DCP pattern and intensity to be similar to the present climate, while the far future indicates an increase in precipitation intensity between 03:00 and 12:00 UTC in 8 of the 12 subdomains analyzed.

KEY WORDS: Diurnal cycle of precipitation · Satellite products · South America · Future scenarios

1. INTRODUCTION

Several studies have documented that the diurnal cycle of precipitation (DCP) over tropical and subtropical land areas is governed by the solar heating of the land surface, which induces atmospheric instability during the day and, eventually, precipitation from mid- to late afternoon (e.g. Kousky 1980, Garreaud & Wallace 1997, Janowiak et al. 2005, Kikuchi & Wang 2008). On the other hand, during the night, the precipitation over land reaches a minimum. Over the open oceans, the peak of precipitation occurs from late evening to early morning hours (e.g. Randall et al. 1991, Imaoka & Spencer 2000, Yang & Slingo 2001, Bowman et al. 2005, Janowiak et al. 2005, Kikuchi & Wang 2008). A short review of some theories that try to explain the pattern of the DCP over the oceans is presented by Janowiak et al. (2005).

The patterns of the DCP mentioned above are only a general view, for they can vary over different regions due to the local dynamics and thermodynamics of each area. In South America (SA), most studies about the behavior of the DCP have focused on the Amazon region (Cutrim et al. 2000, Mota 2003, Mapes et al. 2003, Angelis et al. 2004, Santos Silva 2013, Brito & Oyama 2014, Ferreira et al. 2014) and on northeastern Brazil (Kousky 1980, Teixeira 2008, Brito & Oyama 2014). Over the northern Amazon, the precipitation maximum occurs during the night; over the eastern Amazon, it occurs from late night to early

*Corresponding author: reboita@unifei.edu.br

morning, and over the southern, central, and central-western Amazon, it occurs in the afternoon. It has been suggested that precipitation propagates from the eastern towards the central Amazon (Angelis et al. 2004, Janowiak et al. 2005). One pioneer study about the DCP over northeastern Brazil was developed by Kousky (1980) for the period 1961–1970. For other parts of SA there are fewer studies in the literature about the DCP. Berbery & Collini (2000) reported that the low-level jet east of the Andes has a nighttime maximum that favors increased moisture flux convergence in southeastern SA (north-northeastern Argentina, Paraguay, Uruguay, and southern Brazil), which in turn contributes to the nighttime precipitation. Other studies (Salio et al. 2007, Saulo et al. 2007, Durkee & Mote 2010) indicated that the humidity transported by the low-level jet is the 'fuel' to the mesoscale convective systems (MCSs) in southeastern SA. Janowiak et al. (2005) verified, for the austral summer, the occurrence of an afternoon maximum in precipitation over central and eastern Brazil, a nocturnal maximum in precipitation over areas just east of the Andes (western Argentina, central Bolivia, and western Paraguay), and a late night/early morning maximum over the Atlantic Ocean in the vicinity of the South Atlantic Convergence Zone (SACZ). Note that hereafter, all times shown will be in UTC.

The study of the DCP is not only important to help weather forecasting, but also to evaluate the ability of the numerical models to predict the climate. Comparisons among the DCP from observations and simulations may provide a good opportunity for testing the fundamental physical processes in climate models, including cloud physics, cloud–radiation interactions, air–sea and air–land interactions, as well as small- and large-scale interactions (Kikuchi & Wang 2008). Moreover, models for which simulation of the DCP is similar to observations are more able to reproduce extreme events. Lin et al. (2000) compared the DCP observed over the tropics with simulations by the Colorado State University General Circulation Model. They found that the model did not properly simulate the diurnal cycle or the monthly mean climate state. Dai (2006) verified that the DCP starts too early in several coupled climate models. Dirmeyer et al. (2012) investigated the effects of horizontal resolution and the convection parameterization on the DCP in 7 global model simulations during the austral winter. Generally, there are some improvements in the ability of the models to simulate the DCP as horizontal resolution is increased from 125 to 39, 16, and 10 km.

Considering regional models, Warner et al. (2003) used the fifth-generation Pennsylvania State University–NCAR Mesoscale Model (MM5) to study precipitation over northwestern SA. The results showed that over the Amazon River basin, diurnally initiated rainbands propagate westward, crossing the basin in 2–3 d, which agrees with the observations. Dai et al. (1999) and da Rocha et al. (2009) evaluated the DCP simulated by the Regional Climate Model (RegCM). The former used the model over the US while the latter used it over SA. da Rocha et al. (2009; hereafter R09) simulated 17 summers (1988–2004) between 5 and 35° S. The major similarities, regarding the diurnal cycle phase, between the simulation and the Tropical Rainfall Measuring Mission (TRMM-2A25-PR) observation dataset are found over the continental tropical and subtropical SACZ regions, which present afternoon maximum (15:00–18:00 UTC) and morning minimum (09:00–12:00 UTC). An interesting result obtained by R09 is that RegCM version 3 (RegCM3) does not trigger the moist convection just after sunrise over the southern Amazon and thus does not anticipate the peak of precipitation as reported in global models.

As R09 indicated that RegCM3 performed well in simulating the DCP over SA, and as few studies have assessed the diurnal cycle of this variable in the future climate, the purpose of this study was to analyze the diurnal cycle of precipitation over SA simulated with RegCM4 nested in the outputs of the HadGEM2-ES (Martin et al. 2011) global model for the present climate and the future climate considering the Representative Concentration Pathway (RCP) 8.5 from the Intergovernmental Panel on Climate Change (IPCC). The analysis will consider 3 time-slices: historical (1998–2005), near future (2020–2048), and far future (2070–2098) climates during austral summer (DJF) and winter (JJA). As few studies show a comparison among satellite data, we validated the RegCM4 simulations with the Global Satellite Mapping of Precipitation (GSMaP MVK+) and the TRMM-2A25-PR and TRMM-3B42 datasets. The analysis will contribute to a better understanding of the behavior of these data over SA.

2. DATA AND METHODOLOGY

2.1. RegCM4 and simulation setup

RegCM4 is described by Giorgi et al. (2012) and represents an update of RegCM3 (Pal et al. 2007). Basically, RegCM4 solves the equations for a compressible and hydrostatic atmosphere in finite differences using the sigma-pressure vertical coordinate. As pre-

sented by Giorgi et al. (2012), RegCM4 has many options for the physical parameterization schemes, but here we will only mention those schemes used in the simulation.

Biosphere-Atmosphere Transfer Scheme (BATS, Dickinson et al. 1993), Holtslag planetary boundary layer scheme (Holtslag et al. 1990), and mixed convection (Emanuel over the ocean and Grell over the land; Giorgi et al. 2012) were the parameterizations used in the RegCM4 simulation. The Grell convection scheme was used with Fritsch and Chappell closure. The simulation covers the period from 1970–2098 and is analyzed in 3 time-slices: 1998–2005 (present), 2020–2048 (near future), and 2070–2098 (far future).

The climate simulation used in this study is part of the Phase I CORDEX RegCM4 hyper-Matrix (or CREMA) experiment. As described by Giorgi (2014), CREMA is a project in which RegCM4 is nested in different outputs from the Coupled Model Intercomparison Project phase 5 (CMIP5, Meehl & Bony 2011) general circulation models. From CREMA, we analyzed the simulation in which RegCM4 was nested in HadGEM2-ES (Martin et al. 2011) over the SA CORDEX domain (Fig. 1) and considering the historical experiment for the present climate and the RCP8.5 (Riahi et al. 2011) for the future projections. The simulation used grid spacing of 50 km and 18 sigma-pressure levels.

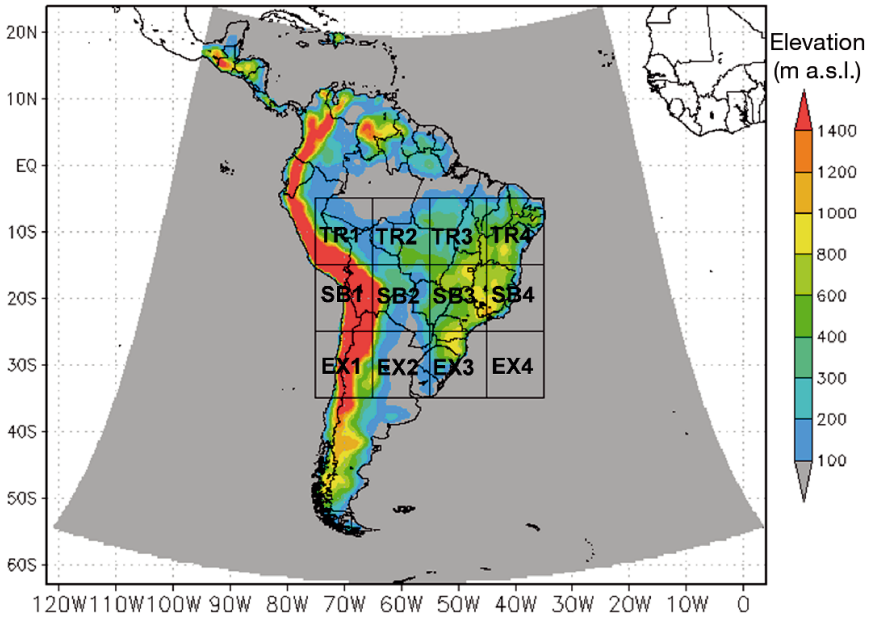

Fig. 1. Domain (gray) and topography (color) used in the RegCM4 simulation. The squares represent the subdomains employed to evaluate the diurnal cycle of precipitation over South America. TR: tropical subdomain, SB: subtropical subdomain, EX: extratropical subdomain

2.2. Observational data

Before describing the dataset used in the present study, it is important to highlight some results of Dai et al. (2007). These authors compared the DCP from CMORPH, PERSIANN, TRMM-3B42, and microwave-only product with surface synoptic weather reports. The authors showed that the products that use infrared (CMORPH, PERSIANN, and TRMM-3B42) do not change the mean frequency and intensity of precipitation; however, they measure the time of maximum precipitation with a lag of a few hours (approximately 2 h). This problem occurs because infrared sensors measure brightness temperatures of cold cloud tops that are often associated with deep convection while the microwave sensors are sensitive to the hydrometeors within clouds. Thus, the products that use infrared do not register the time with maximum total of precipitation; instead they register the time of convective precipitation (deep clouds).

The performance of the satellite products depends on the region of the globe (Janowiak et al. 2005, Demaria et al. 2011, Prakash et al. 2016). Although these data have uncertainties, the satellite products are important to studies on DCP because they cover remote areas and have a good frequency (3 h) and high spatial resolution.

The datasets used in the study are described below.

GSMAP: According to Prakash et al. (2016), the GSMaP project was promoted by the Core Research for Environmental Science and Technology (CREST) of the Japan Science and Technology Agency during 2002–2007 and is now maintained by the Japan Aerospace Exploration Agency Precipitation Measuring Mission. GSMaP is a combination of microwave and infrared satellite observations (Kubota et al. 2007). There are 3 datasets: near real time (GSMaP-NRT) and delayed mode (GSMaP-MVK and GSMaP-MVK+). The difference between GSMaP-MVK and GSMaP-MVK+ is that the former does not use rainfall estimates from the Advanced Microwave Sounding Unit B (AMSU-B) products provided by NOAA (http://sharaku.eorc.jaxa.jp/GSMaP_crest/gdac/doc/GSMaP_MVK+_e.html). In this study, we used GSMaP-MVK+ (hereafter GSMaP) from the period

during which the project was conducted by CREST (2003–2006). GSMaP features are described in Table 1. In the DCP study, the 3-hourly precipitation rate was computed as the mean over the prior 3 h (for example, the 03:00 UTC precipitation is the mean from 00:00 to 03:00 UTC).

TRMM: According to Huffman et al. (2007), TRMM data are constructed by blending precipitation-related passive microwave data collected by a variety of low earth orbit satellites, including the Microwave Imager on TRMM, the Advanced Microwave Scanning Radiometer for Earth Observation System on Aqua, the AMSU-B, and the Special Sensor Microwave Imager. TRMM has different products including TRMM-3B42 (hereafter TRMM) and TRMM-2A25-PR (hereafter TRMM-2A25). TRMM-2A25 is a product based only on the Precipitation Radar, while TRMM-3B42 (version 7) includes infrared precipitation. In the present study, we did not compute the TRMM-2A25 DCP; instead we used the values computed by R09 for the period 1998–2002. Because previous studies (e.g. Dai et al. 2007) have shown that TRMM-3B42 delays the phase of the diurnal cycle, in the present study we shifted the DCP by minus 3 h, i.e. data from 06:00 UTC are considered to be from 03:00 UTC and so on. A summary of the TRMM data is presented in Table 1.

CMAP: Merged Analysis Precipitation (CMAP; Xie & Arkin 1997) is constructed by merging gauge observations, estimates inferred from a variety of satellite observations, and NCEP-NCAR reanalysis. CMAP has horizontal resolution of 2.5°, monthly frequency, and covers the whole globe (land and ocean). CMAP is used in this study in order to compare the seasonal cycle of precipitation over SA among different datasets (GSMaP and TRMM).

2.3. Steps of the study

In the first part of the results, we verify the performance of GSMaP and TRMM over 12 subdomains in SA (Fig. 1), comparing their seasonal precipitation cycle with CMAP. The subdomains follow those presented by R09 and comprise 3 sectors (tropical, subtropical, and extratropical) with 4 subdomains in each sector. We also describe the spatial pattern of the DCP during austral summer and winter observed in GSMaP and TRMM and the possible explanation of the hours with maximum precipitation. It is worth noting that assigning a cause to the differences between GSMaP and TRMM is beyond the scope of this study. In the second part of the study, we use the

Table 1. Characteristics of the datasets used in the study. RegCM4 simulation includes Radiative Concentration Pathways (including greenhouse gas emissions) commencing 2006, and thus 2006 onwards is considered future climate

Dataset	Spatial coverage	Horizontal resolution	Temporal resolution	Temporal coverage	Period used	URL
CMAP	88.75°S – 88.75°N	2.5° × 2.5°	Monthly	1979–present	1998–2005	www.esrl.noaa.gov/psd/data/gridded/data.cmap.html
GSMaP	59.95°S – 59.95°N	0.1° × 0.1°	1 hourly	2003–2006	2003–2006	http://sharaku.eorc.jaxa.jp/GSMaP_crest/gdac/doc/GSMaP_MVK+_e.html
TRMM-2A25	38° S – 38° N	4.3 km until Aug 2001 and 5 km after	3 hourly	Dec 1997–Aug 2001, Aug 2001–present	1998–2002	http://disc.sci.gsfc.nasa.gov/precipitation/documentation/TRMM_README/TRMM_2A25_readme.shtml
TRMM-3B42	50° S – 50° N	0.25° × 0.25°	3 hourly	Dec 1997–Jun 2011	1998–2005	http://mirador.gsfc.nasa.gov/
RegCM Present	60° S – 20° N	0.5° × 0.5°	3 hourly	1970–2005	1998–2005	–
RegCM Near	60° S – 20° N	0.5° × 0.5°	3 hourly	2006–2050	2020–2048	–
RegCM Far	60° S – 20° N	0.5° × 0.5°	3 hourly	2051–2098	2070–2098	–

satellite data to validate the DCP simulated by RegCM4 in the present climate. Moreover, we compare the DCP from satellite products obtained in the present study with that from TRMM-2A25 presented in R09. The DCP obtained for the present climate by RegCM4 will also be compared with the DCP obtained by RegCM3 in R09. The RegCM3 simulation has the same configuration as RegCM4 presented here, but different initial and boundary conditions. While in the present study RegCM4 is nested in HadGEM2-ES, in R09 RegCM3 was nested in the NCEP-Department of Energy reanalysis (Kanamitsu et al. 2002), covering the period 1998–2002. We also discuss the source of precipitation (convective or large scale) by computing the ratio between convective and total precipitation. Finally, the DCP in the RCP8.5 scenario for near (2020–2048) and far (2070–2098) future climates is presented.

3. RESULTS

3.1. Seasonal cycle of precipitation

This section presents a comparison of the seasonal cycle of precipitation among GSMaP, TRMM, and CMAP over the 12 subdomains shown in Fig. 1. In almost all subdomains (Fig. 2), the 3 datasets present higher values of precipitation in summer (DJF) and lower values in winter (JJA); the exceptions are in EX3, where GSMaP has lower precipitation in summer, and in EX4, where TRMM has lower precipitation in spring (SON).

Considering all subdomains, the values of seasonal precipitation are more similar between TRMM and CMAP, while GSMaP shows, in general, an underestimation of about 1 mm d^{-1}. Even though there are some differences in the precipitation values among

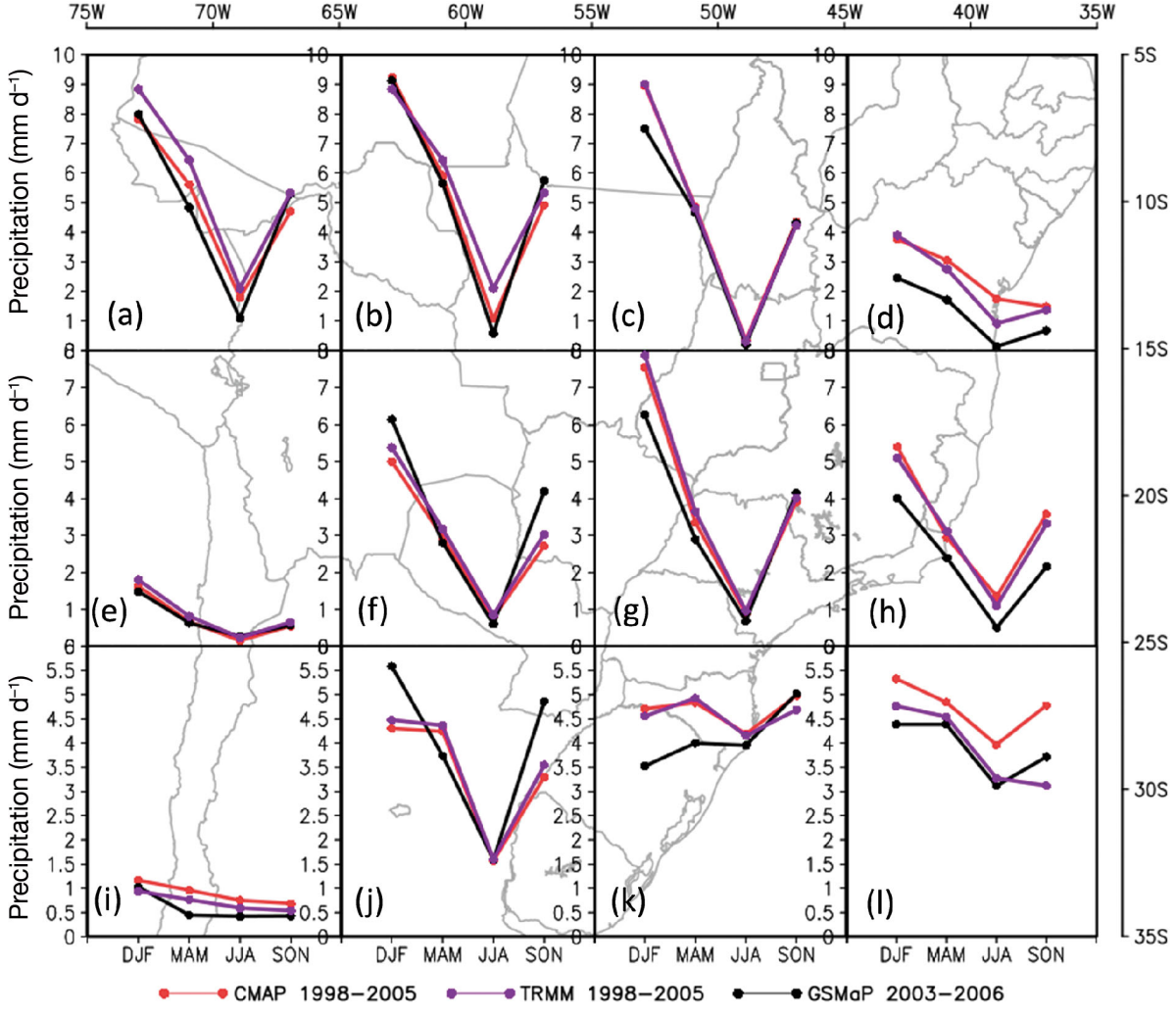

Fig. 2. Seasonal cycle of precipitation over the 12 subdomains (a–l) shown in Fig. 1 obtained with CMAP (1998–2005; red line), TRMM-3B42 (1998–2005; purple line), and GSMaP-MVK+ (2003–2006, black line)

the 3 datasets, they all show a similar seasonal cycle of precipitation. These results are consistent with Dai et al. (2007), who mentioned that the satellite products have a monthly mean precipitation amount comparable to other monthly products such as CMAP and Global Precipitation Climatology Project (GPCP) (which include rain-gauge data). This is indicative of the reliability of the satellite products and, therefore, we used these products to validate the DCP simulated over SA by RegCM4.

3.2. Spatial pattern of the diurnal cycle of precipitation in TRMM and GSMaP

The spatial pattern of the DCP over most of SA in austral summer registered in TRMM and GSMaP is shown in Figs. 3 & 4, respectively. In the previous section, it was indicated that TRMM is rainier than GSMaP. During the day, the hours that contributed most to this feature of TRMM are 15:00 and 18:00 UTC. Even though there are some differences in the precipitation values between TRMM and GSMaP in each hour, the spatial pattern of precipitation (areas with higher and lower values) is very similar in both datasets (Figs. 3 & 4).

In summer (Figs. 3 & 4), from the Amazon basin to southeastern Brazil, higher precipitation totals occur between 15:00 and 21:00 UTC (Figs. 3f–h & 4f–h) while lower totals occur at 12:00 UTC (Figs. 3e & 4e). The precipitation daytime maximum is associated with the surface heating (convective processes; Janowiak et al. 2005, R09) and the SA Monsoon (SAM; Vera et al. 2006, Reboita et al. 2010a, Marengo et al. 2012). In this region, TRMM is rainier than GSMaP at 15:00 and 18:00 UTC.

In coastal areas over the northern portion of the north and northeast regions of Brazil, the daytime heating and the influence of the sea breeze can develop precipitation in the form of squall lines (Garstang et al. 1994, Cohen et al. 1995, Teixeira 2008). This line of rainfall starts at 15:00 UTC and produces the maximum of precipitation around 3 h later, at 18:00 UTC, extending along a line parallel to the coast (Figs. 3g & 4g). After this time, this line remains intense and is displaced inland (to the southwest). According to Cohen et al. (1995), Janowiak et al. (2005), and Garreaud & Wallace (1997), the precipitation line advances, producing nighttime-predawn maxima approximately 500 km from the coast. This feature is also very clear in TRMM and GSMaP (Figs. 3a–d & 4a–d). Comparing both of these datasets, along the northern and northeastern

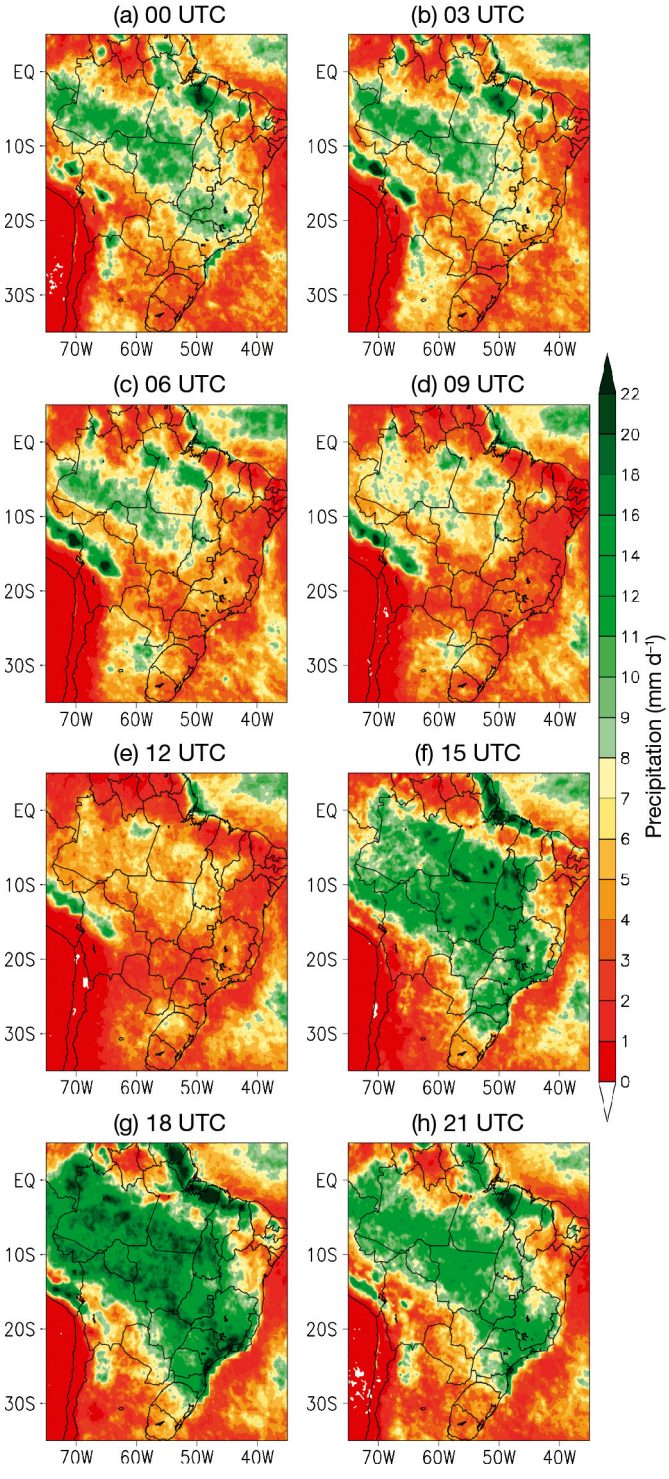

Fig. 3. Spatial pattern of the diurnal cycle of precipitation (mm d^{-1}) every 3 h in austral summer (1998–2005) from TRMM-3B42: (a) 00:00, (b) 03:00, (c) 06:00, (d) 09:00, (e) 12:00, (f) 15:00, (g) 18:00, and (h) 21:00 UTC

Brazilian coast, TRMM is rainier than GSMaP. A maximum of precipitation, also associated with the sea breeze (for example, Freitas et al. 2007), occurs in

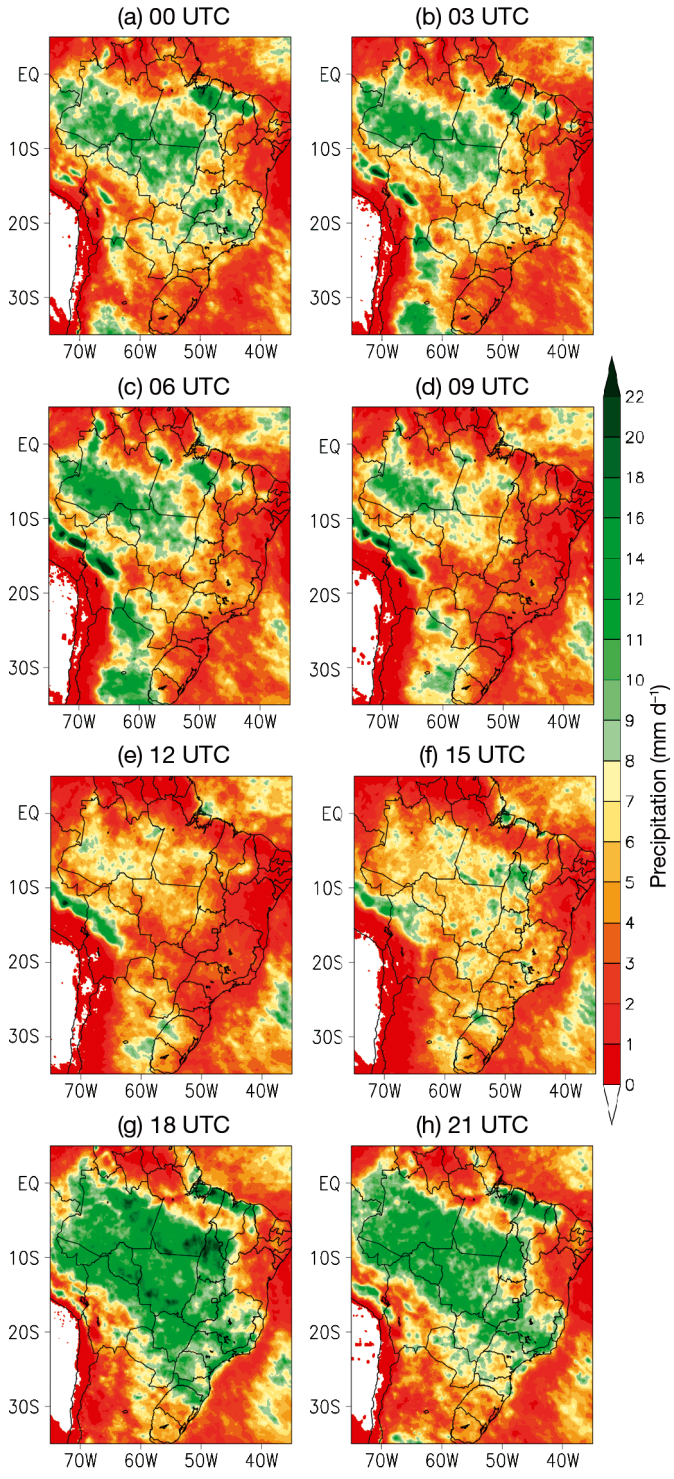

Fig. 4. As in Fig. 3, but with GSMaP-MVK+ (2003–2006)

the south-southeastern coast of Brazil between 18:00 and 21:00 UTC (Figs. 3g,h & 4g,h). The breezes in the coast of southern and southeastern Brazil are less documented than in the northern and northeastern regions.

Over the eastern border of the Andes Mountains (Bolivia and Peru), the maximum of precipitation is registered between 06:00 and 09:00 UTC (Figs. 3c,d & 4c,d). TRMM and GSMaP show similar precipitation values. Using infrared images, Garreaud & Wallace (1997) proposed that the nocturnal maximum over the eastern border of the Andes is a result of the convergence between the nighttime downslope mountain flow and the predominant northeasterly wind over the western Amazon basin. Such a mechanism was evident in the model results of R09.

Over the border of Argentina and Bolivia, the maximum of precipitation occurs between 21:00 and 03:00 UTC (Figs. 3a,b,h & 4a,b,h), which is normally attributed to the nocturnal development of MCSs (Velasco & Fritsch 1987, Mohr & Zipser 1996, Laing & Fritsch 1997, Saulo et al. 2007, Salio et al. 2007). In general, MCSs originate downstream of the low level jet east of the Andes Mountain (Silva Dias et al. 1987). These convective systems have a short lifetime (~12 h) and normally move to the east reaching southern Brazil. Due to this feature, the maximum of precipitation in the western boarder of Paraguay, Uruguay, and extreme southern Brazil occurs between 06:00 and 09:00 UTC (Figs. 3c,d & 4c,d). In this sector, TRMM and GSMaP show differences. The precipitation in GSMaP is higher than in TRMM and covers a larger area from the southern domain of Figs. 3c,d & 4c,d to southern Bolivia. Finally, the main features of the spatial pattern of the DCP over SA registered in TRMM and GSMaP during summer agree with the ones from CMORPH analyzed by Janowiak et al. (2005).

In general, the literature focuses on the study of the DCP during the warm season (e.g. R09). Here, we complement the literature by showing the DCP analysis over SA during winter. In both TRMM (Fig. 5) and GSMaP (Fig. 6), precipitation totals in winter decrease compared to summer due to the weakening of the surface warming and the SAM. Higher precipitation totals concentrate over northwestern SA and over southern Brazil. Most of SA has precipitation below 1 mm d^{-1}. In winter, TRMM is also rainier than GSMaP in some parts of SA, viz. northwestern SA and northeastern Brazil. In the latter region, the precipitation reaches 0 mm d^{-1} in GSMaP. Moreover, this is the driest region over SA in winter.

Over northwestern SA, the maximum of precipitation occurs between 18:00 and 21:00 UTC (Figs. 5g,h & 6g,h) and is associated with convective activity. On

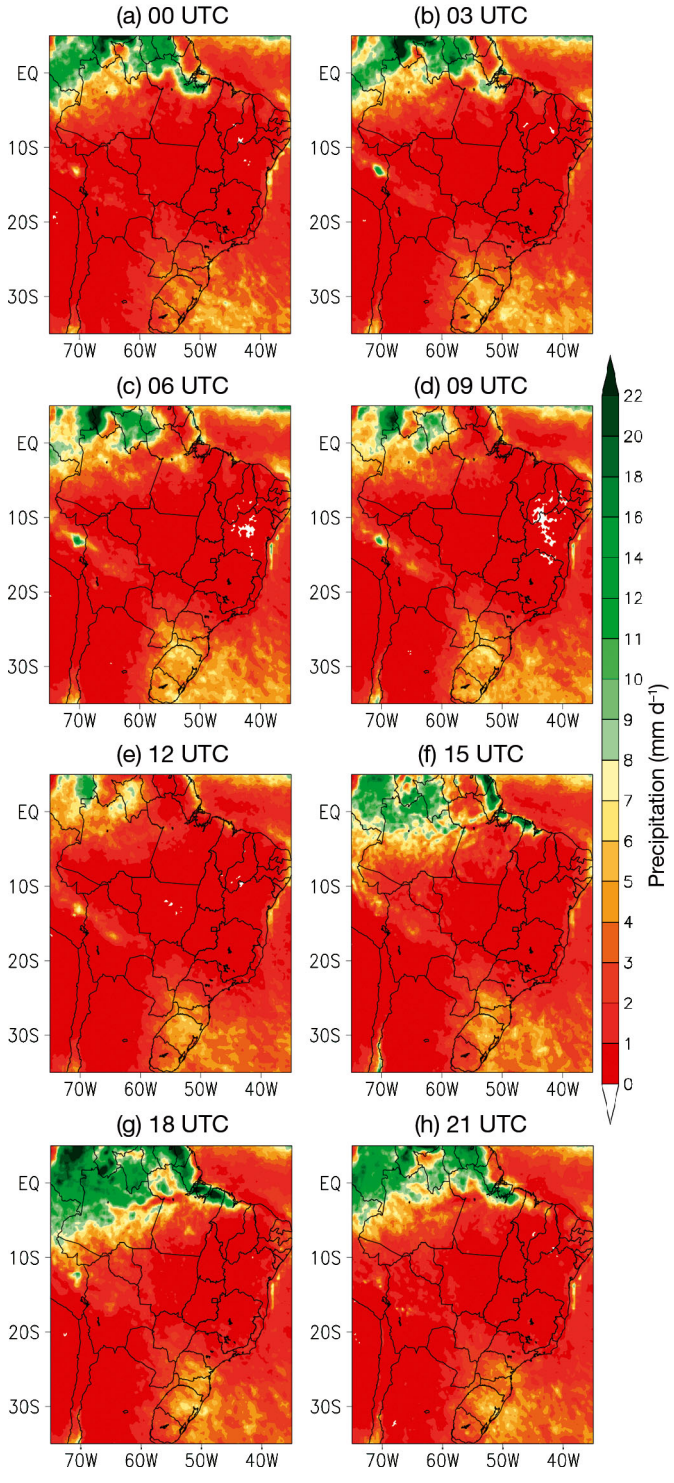

Fig. 5. As in Fig. 3, but for austral winter with TRMM-3B42 (1998–2005)

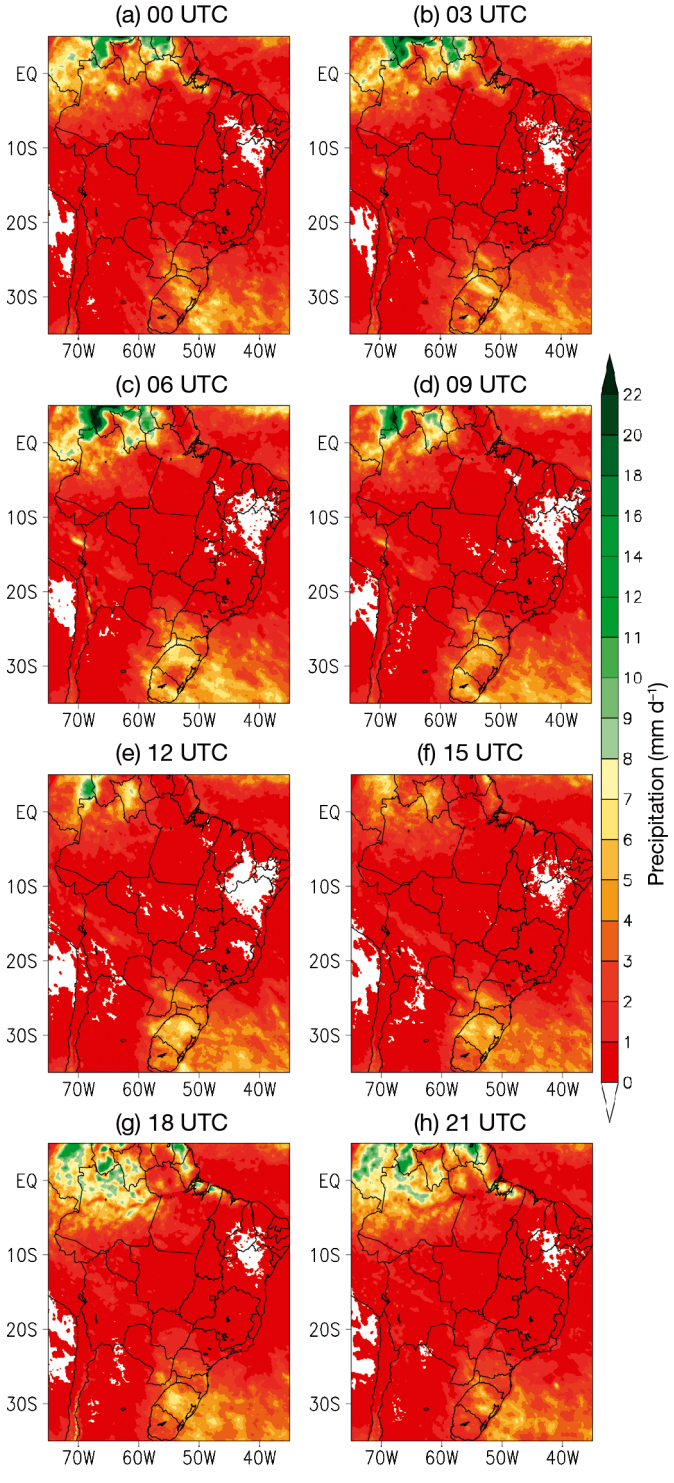

Fig. 6. As in Fig. 3, but for austral winter with GSMaP-MVK+ (2003–2006)

the other hand, over southern Brazil precipitation is more evenly distributed across the DCP. As this region is continually influenced by frontal systems (Satyamurty & Mattos 1989, Reboita et al. 2009) and extratropical cyclones (Reboita et al. 2010b, 2012) and because these systems do not reach the region at any distinct time, the precipitation becomes well distributed across the DCP.

3.3. Subdomain analyses

3.3.1. Austral summer

Tropical subdomains. Fig. 7 shows the observed and simulated (present and future scenarios) DCP during summer considering the total precipitation, while Fig. 8 shows the ratio between convective and total precipitation. This ratio allows the identification of the precipitation source: convective or large scale. In Fig. 7, the gray line shows the DCP obtained by R09, considering TRMM-2A25 data for the summer season from 1998–2002.

GSMaP, TRMM, and TRMM-2A25 indicate that in the tropical region (15–5° S) the precipitation maximum occurs at 18:00 UTC over the 4 subdomains (Fig. 7a–d) and a secondary maximum occurs between 03:00 and 06:00 UTC in TR1. The highest differences between satellite products occur over TR1, where TRMM-2A25 (R09; see Fig. 7 in that study and the gray line in Fig. 7 of the present study) is drier than GSMaP and TRMM. In TR4, TRMM-2A25 shows a slight maximum at 06:00 UTC that is not present in GSMaP and TRMM. Moreover, studies with CMORPH (Janowiak et al. 2005, Pereira Filho et al. 2014, 2015) also do not show this peak at 06:00 UTC.

In general, in the tropical subdomains (Fig. 7a–d), RegCM4 simulates for the present climate lower precipitation than GSMaP and TRMM from 00:00 to 06:00 UTC and higher than GSMaP from 15:00 to 21:00 UTC. However, the maximum precipitation

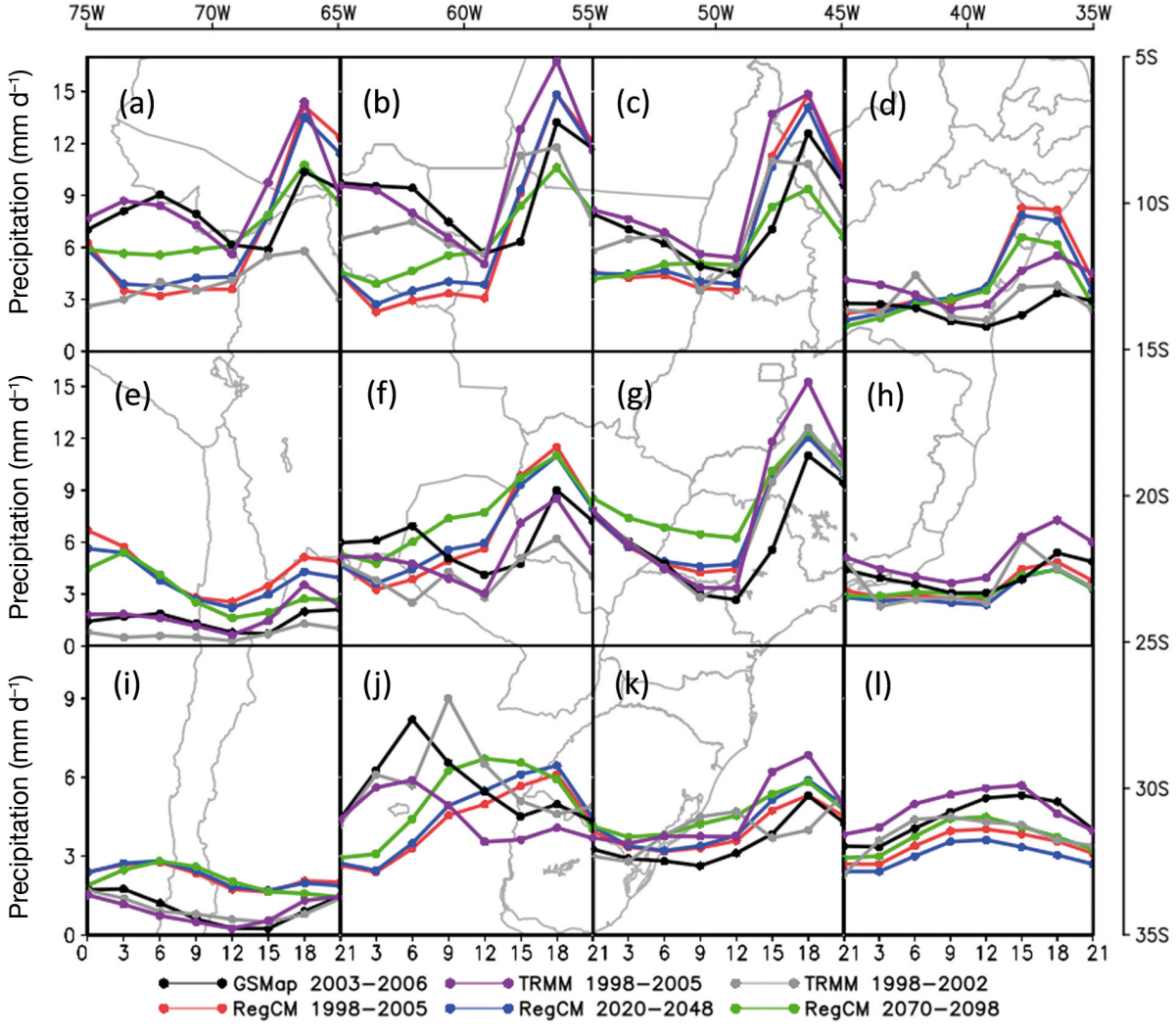

Fig. 7. Diurnal cycle of total precipitation over the 12 subdomains (a–l) shown in Fig. 1 in austral summer and obtained with GSMaP-MVK+ (2003–2006, black line), TRMM-3B42 (1998–2005, purple line), TRMM-2A25 (1998–2002; from da Rocha et al. 2009, gray line), RegCM4 present climate (1998–2005; red line), RegCM4 near future (2020–2048; blue line), and RegCM4 far future (2070–2098; green line)

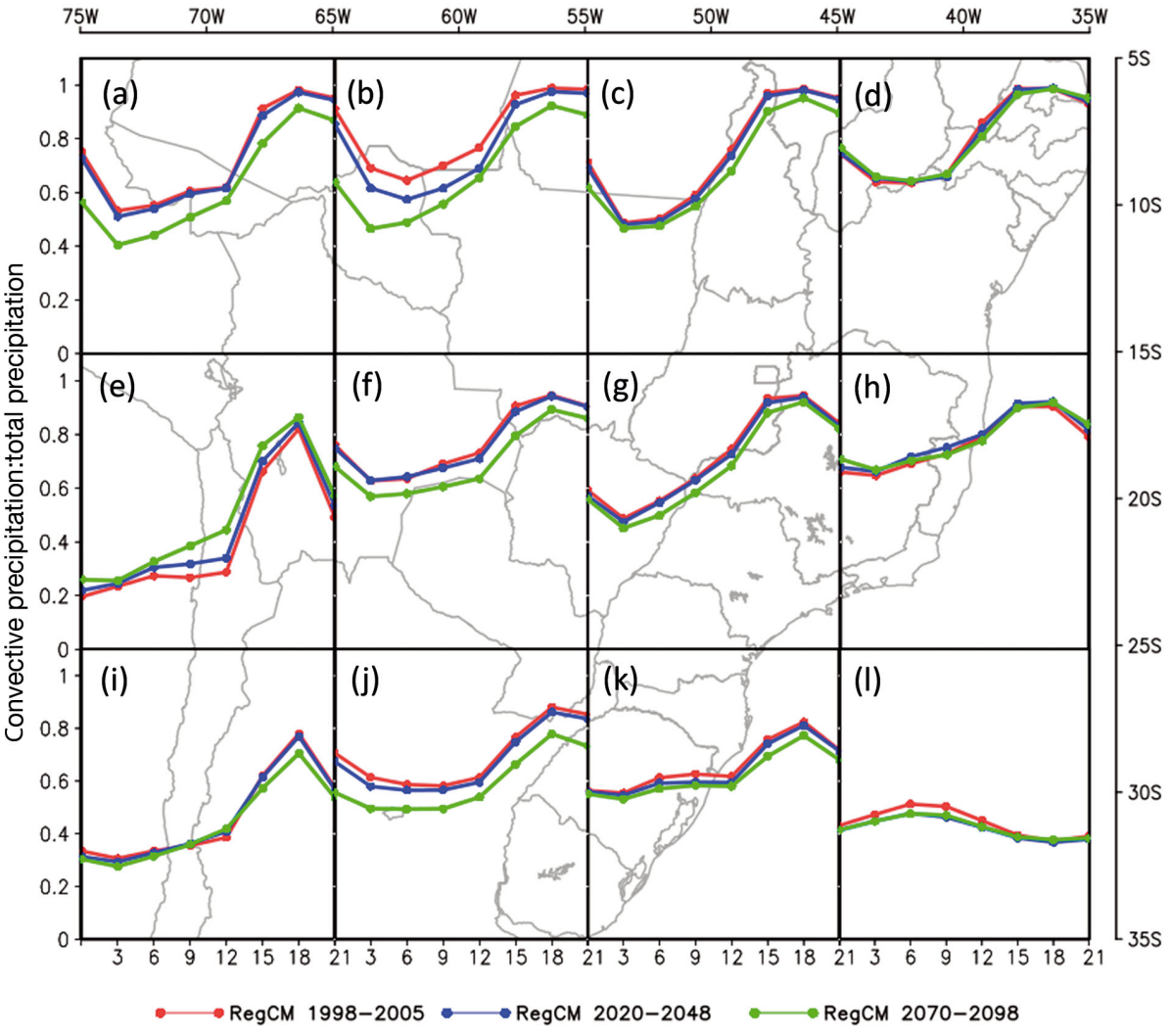

Fig. 8. Ratio of convective precipitation to total precipitation in austral summer simulated by RegCM4 in the present (red line) and near- and far-future climates (blue and green lines, respectively)

simulated at 18:00 UTC is close to TRMM in TR1 and TR3. RegCM3 (R09; their Fig. 7) also simulated, in general, the precipitation peak at 18:00 UTC. This result indicates a good performance of RegCM4 compared with global climate models (Lin et al. 2000, Dai 2006, Ma & Mechoso 2007), which displace the peak of precipitation to the morning. For example, Ma & Mechoso (2007) verified that the University of California, Los Angeles, atmospheric global model simulates the precipitation maximum in the morning instead of in the afternoon over tropical SA.

According to Fig. 8a–d, in the tropical subdomains the precipitation is mostly of convective origin, mainly from 15:00 to 21:00 UTC when the ratio of convective to total precipitation is approximately 1. These results are consistent with R09. In addition, R09 showed that RegCM3 underestimated the convective precipitation from 00:00 to 06:00 UTC and overestimated it from 15:00 to 18:00 UTC (compared with TRMM-2A25) and highlighted that it is a systematic error that occurs in several RegCM versions.

Regarding the future scenarios, the near-future climate does not show changes in the pattern and intensity of the DCP. However, the far scenario projects a precipitation increase from 03:00 to 12:00 UTC in TR1 and TR2 (Fig. 7a,b) and from 06:00 to 12:00 UTC in TR3 (Fig. 7c). Precipitation decreases from 18:00 to 21:00 UTC in TR1 and TR2 and from 15:00 to 21:00 UTC in TR3 and TR4. In summary, in the driest (rainiest) hours during the day in the present climate, RegCM4 projects an increase (decrease) of precipitation in the far scenario.

Subtropical subdomains. In the subtropical region (25–15° S), maximum precipitation occurs at 18:00

UTC in both TRMM and GSMaP (Fig. 7e–h). However, some differences between the satellite products are verified. In SB2 (Fig. 7f), GSMaP shows a secondary maximum of precipitation at 06:00 UTC that should be associated with MCSs (Fig. 4c). This peak does not appear in TRMM while in TRMM-2A25 it occurs at 09:00 UTC. In SB4, in the present study (Fig. 7h), GSMaP and TRMM have a similar DCP phase, but it is different in TRMM-2A25, in which the DCP has a main maximum at 15:00 UTC and a secondary one at 00:00 UTC.

Regarding the present simulation, RegCM4 overestimates the precipitation values compared with the satellite products, except in SB4 (Fig. 7h), where the values are more similar to the observations. In this subdomain and SB3 (Fig. 7g), the pattern of DCP is also similar to the observation. R09 also showed good performance of RegCM3 in SB3. These authors indicated that SB3 includes most of the SACZ and that the afternoon precipitation maximum is probably the result of the strong solar heating at the surface and the sea-breeze circulation associated with the steep coastline in the region.

Some of the differences between model and observations, which are worth mentioning, occur in SB1 and SB2. In SB1 (Fig. 7e), the model simulates the main precipitation peak at 00:00 UTC and a secondary peak at 18:00 UTC, while in the observations the precipitation maximum occurs at 18:00 UTC. The excessive precipitation simulated during the night and early morning in SB1 can be associated with the large-scale precipitation (grid-scale scheme), as indicated in Fig. 8e, which shows that the ratio between convective and total precipitation is about 0.2 (20%) and can be a model deficiency. In SB2 (Fig. 7f), RegCM4 does not simulate the secondary maximum of precipitation registered at 06:00 UTC in GSMaP. In this region, the maximum of precipitation at 18:00 UTC observed in all datasets has convective origin while the second one observed in GSMaP can be associated with large-scale and convective processes. SB2 is a region with MCSs (Velasco & Fritsch 1987, Salio et al. 2007, Durkee & Mote 2010, Demaria et al. 2011), and the source of heat and humidity to these systems is the low-level jet east of the Andes, which is a large-scale system. The RegCM4 low skill in SB2 will be discussed together with EX2 in 'Extartropical subdomains', belowc.

Considering the future projections, in SB1 (Fig. 7e) both near- and far-future scenarios indicate a decrease in the precipitation intensity from 12:00 to 00:00 UTC with the highest changes occurring in the far scenario when compared with the present climate. On the other hand, in SB2 and SB3 (Fig. 7f,g), the near scenario projects precipitation values similar to the present, while the far scenario projects an increase in precipitation between 03:00 and 12:00 UTC. The increase in precipitation in these subdomains, which correspond to a large part of the La Plata Basin, is also obtained by different regional climate models in the future (e.g. Solman et al. 2013, Llopart et al. 2014, Reboita et al. 2014, Mourão et al. 2016). In SB4 (Fig. 7h), both near and far scenarios simulate precipitation values similar to the present climate.

Extratropical subdomains. In the extratropical region (35–25° S), the peaks of precipitation occur in different periods in each subdomain, as shown in Figs. 7i–l, and RegCM4 only represents well the pattern of the DCP in EX3 when compared to GSMaP and TRMM. When compared to TRMM-2A25, as in R09, the model shows poor performance over all extratropical subdomains. It is interesting to mention that in EX4, the pattern of DCP in TRMM and GSMaP is similar to that in CMORPH (Janowiak et al. 2005).

In EX1 (Fig. 7i), the model overestimates the satellite products. In terms of precipitation source, RegCM4 indicates that in EX1 the precipitation between 00:00 and 12:00 UTC is more associated with large-scale mechanisms and in the following hours with convection (Fig. 8i). In EX1 and SB1, the low values of precipitation found in the DCP of the satellite products are likely associated with the influence of the South Pacific Subtropical Anticyclone (Garreaud & Falvey 2009); subsidence inhibits convection.

In both SB2 (Fig. 7f) and EX2 (Fig. 7j), the different RegCM versions (see RegCM3 in R09) underestimate the precipitation at 06:00 UTC. Although the precipitation in these regions is mainly associated with convection (Fig. 8f,j), the humidity used in the convective process is transported by a large-scale system, i.e. the low-level jet at the east side of the Andes Mountains. This jet transports heat and humidity from tropics to higher latitudes, contributing to the development of MCSs. As shown by Reboita et al. (2010a,b) and Llopart et al. (2014), the underestimation of the low-level jet meridional winds is a systematic error in different versions of RegCM, and can explain the lower precipitation simulated at 06:00 UTC compared with the observations. In EX3 and EX4, the large-scale precipitation is related to cold fronts (Satyamurty & Mattos 1989, Reboita et al. 2009) and cyclogenesis (Hoskins & Hodges 2005, Reboita et al. 2010b).

Considering the future scenarios, for the near-future climate in all extratropical subdomains (Figs. 7i–l) there is no evident change in the pattern

of the DCP compared to the present climate simulation. For the far-future climate, the pattern of the DCP is also similar to the present climate simulation in both EX1 and EX4 subdomains (Figs. 7i,l), with EX4 showing a slight increase in precipitation from 00:00 to 15:00 UTC. In EX2 and EX3 for the far-future climate (Figs. 7j,k), RegCM4 simulates the highest increases in the precipitation values from 06:00 to 12:00 UTC, and in EX2 the peak of maximum precipitation is displaced to 12:00 UTC instead of 18:00 UTC as in the present climate.

Regarding the projections of the DCP for the far-future scenario in all of the 12 subdomains analyzed, the results shown here are consistent with the seasonal changes presented by Llopart et al. (2014). Those authors used the same RegCM4 simulation to the present and far scenario employed here, and analyzed the changes in the precipitation between December and April. They showed an increase in precipitation in central-southern SA, which is consistent with the increase of precipitation in the far-future simulation (Fig. 7) in 8 out of 12 subdomains (TR1, TR2, TR3 SB2, SB3, EX2, EX3, EX4), mainly between 00:00 and 12:00 UTC. Moreover, other studies such as those by Solman et al. (2013), Reboita et al. (2014), and Mourão et al. (2016), using different models, scenarios, and boundary conditions, also indicate an increase in precipitation in central-southern SA.

3.3.2. Austral winter

An important contribution of this study is the DCP analysis during winter, since references in the literature focus mainly on the summer season. In the aus-

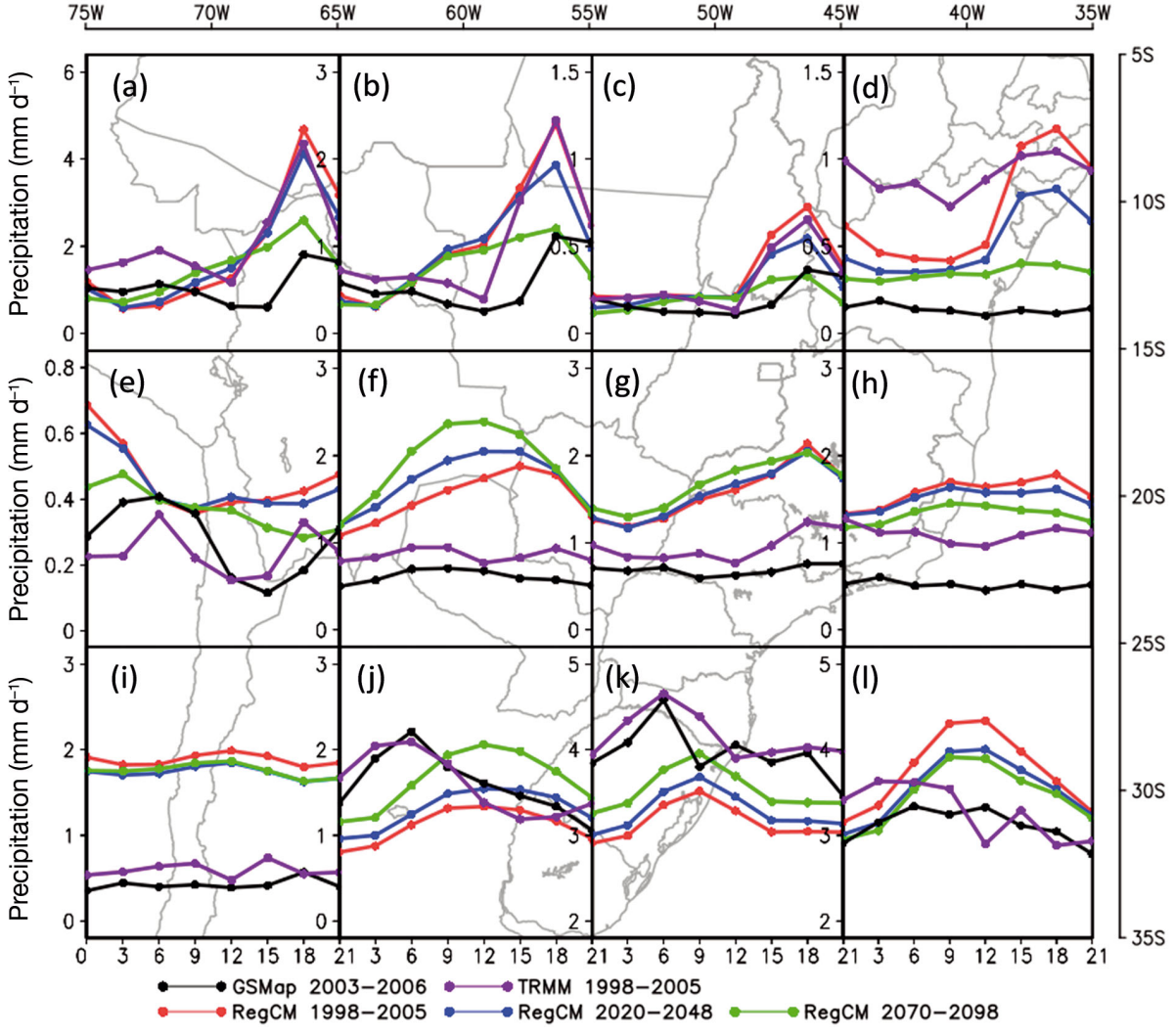

Fig. 9. As in Fig. 7, but for austral winter

tral winter, the solar heating over SA is weaker than in summer and the monsoon systems are also consequently weak. Therefore, during winter there is a drastic decrease in precipitation in a large part of the continent. In that season, the precipitation is concentrated over the northwestern SA (Vera et al. 2006, Reboita et al. 2010a), but there is a secondary maximum centered over southern Brazil, Uruguay, and northeastern Argentina.

Tropical subdomains. During winter in the tropical subdomains, the satellite products show a maximum of precipitation at 18:00 UTC, with GSMaP being drier than TRMM, particularly between 15:00 and 18:00 UTC (Fig. 9a–d). In all tropical subdomains, RegCM4 also indicates that the peak of precipitation occurs at 18:00 UTC (and has a convective origin), but the model overestimates the precipitation values. Regarding the future scenarios, the model projects in the 4 subdomains a decrease in precipitation between 15:00 and 21:00 UTC when compared with TRMM, with this decrease being more intense in the far-future scenario. As the precipitation between 00:00 and 12:00 UTC is near 0 in the tropical subdomains during winter, we can expect only reduction during the afternoon maximum.

Subtropical subdomains. In the subtropical subdomains (Fig. 9e–h), the DCP in TRMM and GSMaP is almost constant throughout the day (in SB1, the pronounced diurnal cycle is an effect of the figure axis), with values about 1 mm d^{-1} (except in SB1 where precipitation values are around 0.5 mm d^{-1}). Therefore, the results described concerning the subtropical subdomains should be interpreted cautiously, bearing in mind that the precipitation intensity is similar to the errors of this variable estimated by the satellite.

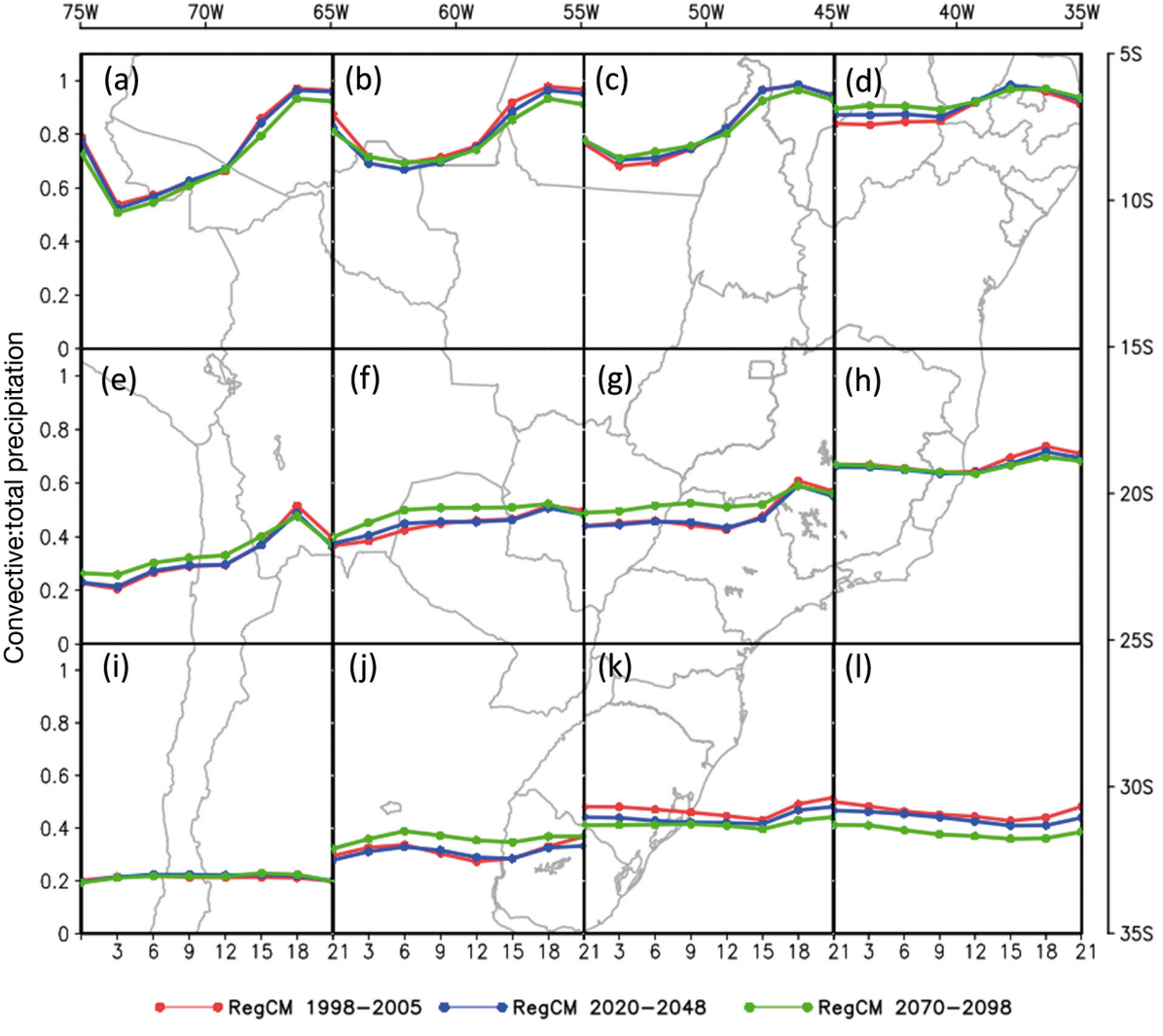

Fig. 10. As in Fig. 8, but for austral winter

In all 4 subtropical subdomains, RegCM4 overestimates the precipitation in the present climate compared with the satellite products, and does not reproduce well the pattern of the DCP. In SB1 (Fig. 9e), RegCM4 shows a peak at 00:00 UTC, in SB2 (Fig. 9f) at 15:00 UTC, in SB3 (Fig. 9g) at 18:00 UTC (this peak is in phase with TRMM), and in SB4 (Fig. 9h) a slight peak is seen at 18:00 UTC. Regarding the precipitation source (Fig. 10e–h), RegCM4 indicates that in SB1, SB2, and SB3 the precipitation is more associated with large-scale processes (precipitation ratio below 0.5), while in SB4 both convective and large-scale processes are important to precipitation.

Regarding the future climate projections, in SB1 and SB4 a slight decrease in precipitation throughout the day is projected. On the other hand, in SB2 and SB3 an increase in precipitation is projected, and this increase is more intense in the far-future in SB2 (Fig. 9f). These results are consistent with the seasonal study of Llopart et al. (2014).

Extratropical subdomains. Considering the extratropical subdomains (Fig. 9i–l), in EX1 the precipitation values are practically constant in both TRMM and GSMaP, with TRMM showing a slight minimum at 12:00 UTC. In that region, RegCM4 overestimates the DCP by about 1.5 mm d^{-1} compared with the satellite products. The model also shows a DCP with constant values throughout the day. In EX2 and EX3 (Fig. 9j,k), RegCM4 underestimates the satellite datasets in the present climate and simulates a delayed maximum of precipitation compared with the observation. On the other hand, in EX4 (Fig. 9l) the model overestimates the precipitation from 06:00 to 21:00 UTC compared with TRMM. While in EX4 the satellite products indicate a slight maximum of precipitation between 03:00 and 06:00 UTC, the model simulates it between 09:00 and 12:00 UTC. This is probably an error of the model, because in that region the systems that contribute to precipitation (fronts and cyclones) do not have a typical hour of occurrence. In all extratropical subdomains, the source of precipitation is more related with large scale processes (Fig. 10i–l).

For the future climate, a decrease in precipitation is projected in EX1 and EX4, with the near- and far-future climates in EX1 showing similar values, and the far-future climate being slightly drier than the near future in EX4. On the other hand, an increase in precipitation is projected in EX2 and EX3 and is more pronounced in the far future. The increase in precipitation in EX2 and EX3 is coherent with other studies that also project increases in precipitation in the La Plata Basin during winter (e.g. Reboita et al. 2014).

4. DISCUSSION AND CONCLUSIONS

This study compared the DCP during austral summer and winter simulated by RegCM4 in the present climate (1998–2005) with TRMM and GSMaP, and showed the projections to the near- and far-future cli-

Table 2. Austral summer summary: hour (UTC) with the peak of precipitation in the present climate, source of precipitation (based on RegCM4), and indication of the diurnal cycle of precipitation period in which an increase in rainfall is projected in the far-future climate. None: no increase in rainfall

	Peak of precipitation (UTC)					Source of precipitation	Increase in rain (UTC) (2070–2098)
	GSMaP	TRMM-3B42	TRMM-2A25	RegCM3	RegCM4		
TR1	18:00	18:00	18:00	18:00	18:00	Convective	03:00–12:00
TR2	18:00	18:00	18:00	18:00	18:00	Convective	03:00–12:00
TR3	18:00	18:00	15:00–18:00	15:00–18:00	18:00	Convective	06:00–12:00
TR4	18:00	18:00	06:00	15:00–18:00	15:00–18:00	Convective	None
SB1	18:00–21:00	18:00	18:00	00:00–03:00	00:00	Large scale and convective	None
SB2	18:00	18:00	18:00	18:00	18:00	Convective	00:00–12:00
SB3	18:00	18:00	18:00	18:00	18:00	Convective	00:00–12:00
SB4	18:00	18:00	15:00	18:00	18:00	Convective	None
EX1	00:00–03:00	18:00–00:00	21:00–03:00	03:00–06:00	00:00–09:00	Large scale and convective	None
EX2	06:00	06:00	09:00	18:00	18:00	Convective	03:00–15:00
EX3	18:00	18:00	21:00	18:00	18:00	Convective	03:00–21:00
EX4	12:00–18:00	09:00–15:00	06:00–09:00	15:00–18:00	09:00–15:00	Large scale	00:00–15:00

mates considering the IPCC RCP8.5 scenario. The simulation was carried out using the HadGEM2-ES outputs as boundaries in RegCM4. Questions about the uncertainty of using only 1 simulation to obtain the DCP projections are expected. However, our purpose is to evaluate the DCP in an individual simulation of CREMA, if the increase in precipitation projected agrees with the regions shown in Llopart et al. (2014).

Tables 2 & 3 summarize the hour of maximum precipitation in GSMaP, TRMM, TRMM-2A25, RegCM3, and RegCM4 over each subdomain and in the present climate, for summer and winter, respectively. Moreover, these tables indicate the source of precipitation and the period of the DCP in which an increase of rain is projected for the future climate.

Over SA, RegCM4 performs better in the tropical subdomains and worse over the extratropical subdomains. The skill over the tropical subdomains is relatively high, since other models (e.g. Liang et al. 2004, Ma & Mechoso 2007) do not represent the afternoon maximum of precipitation. This indicates that convective and grid-scale schemes in RegCM4, as in RegCM3 (R09), respond to different forcing scales: local (diurnal heating), mesoscale (sea–land breeze and mountain–valley circulations), and large scale (SAM systems).

In the tropical and subtropical subdomains, the maximum precipitation in the summer occurs mostly at 18:00 UTC associated with the strong solar heating at the surface that produces large sensible and latent heat fluxes from surface to the lower troposphere which is important in the development of convection. In the extratropical region, the peak of precipitation is different among the subdomains. In SB2 and EX2, TRMM and GSMaP register a secondary precipitation maximum at 06:00 UTC. However, this feature is not simulated by RegCM4. The precipitation source in both subdomains is related to convective and large-scale processes, being associated with MCSs which obtain most of their needed humidity from the large-scale transport of mass from the tropics to higher latitudes provided by the low-level jet east of the Andes. The weaker low-level jet in RegCM4 (a common problem in the different versions of this model) should negatively affect the development of MCSs (a convective process), and thus RegCM4 does not simulate the secondary maximum of precipitation. In winter, precipitation is reduced compared with summer, and RegCM4 simulates this characteristic well. However, when the model is compared with TRMM and GSMaP, it overestimates the precipitation in all subtropical subdomains and in EX1 and EX4.

For the future scenarios, in general, during summer the near future (2020–2048) shows the pattern and intensity of the DCP similar to the present climate, while the far future (2070–2098) projects an increase in precipitation between 03:00 and 12:00 UTC and a decrease in precipitation between 15:00 and 21:00 UTC in 8 of 12 subdomains. The increase in precipitation over the subdomains located in and near the La Plata Basin is consistent with seasonal precipitation projections carried out by different models (Solman et al. 2013, Reboita et al. 2014, Mourão et al. 2016), which indicate a precipitation increase over the La Plata Basin and a precipitation decrease over northern SA. It is interesting to highlight that our tropical subdomain is inside a region of transition between dry and wet conditions in the future.

Table 3. As in Table 2, but for austral winter

	Peak of precipitation (UTC)			Source of precipitation	Increase in rain (UTC) (2070–2098)
	GSMaP	TRMM-3B42	RegCM4		
TR1	18:00–21:00	18:00	18:00	Convective	06:00–12:00
TR2	18:00–21:00	18:00	18:00	Convective	None
TR3	18:00–21:00	18:00	18:00	Convective	None
TR4	No maximum	15:00–00:00	15:00–21:00	Convective	None
SB1	No maximum	No maximum	00:00	Large scale	None
SB2	No maximum	No maximum	15:00	Large scale	00:00–21:00
SB3	No maximum	No maximum	18:00	Large scale	00:00–15:00
SB4	No maximum	No maximum	18:00	Large scale and convective	None
EX1	No maximum	No maximum	No maximum	Large scale	None
EX2	06:00	03:00–06:00	09:00–15:00	Large scale	00:00–21:00
EX3	06:00	06:00	09:00	Large scale	00:00–21:00
EX4	03:00–09:00	03:00–09:00	09:00–12:00	Large scale	No

The final question of the study is whether there are any improvements in using RegCM4 over RegCM3. Comparing our present simulation (RegCM4) with that from R09 (RegCM3), we verified that both RegCM versions have a similar performance. On first impressions, the DCP simulated here by RegCM4 can show better results than the DCP simulated in R09 by RegCM3; however, this is due to the different datasets used for model validation. R09 used only TRMM-2A25 to validate RegCM3; however, we have shown here that TRMM-2A25 has some differences when compared to TRMM-3B42 and GSMaP. Because RegCM4 simulated a DCP similar to TRMM and GSMaP, this indicates that RegCM4 performed well. If R09 used TRMM and GSMaP to validate the DCP from RegCM3, they would have found that RegCM3 also performs well in the simulation of the DCP over SA.

Acknowledgements. We thank the meteorological services for CMAP, TRMM, and GSMaP data; The Abdus Salam International Centre for Theoretical Physics (ICTP) for RegCM4; M. Llopart for carrying out the simulation in ICTP under the scope of the CORDEX project; and CNPq (process number 474929/2013-2) for financial support.

LITERATURE CITED

Angelis CF, McGregor GR, Kidd C (2004) Diurnal cycle of rainfall over the Brazilian Amazon. Clim Res 26:139–149

Berbery EH, Collini EA (2000) Springtime precipitation and water vapor flux over southeastern South America. Mon Weather Rev 128:1328–1346

Bowman KP, Collier JC, North GR, Wu Q, Ha E, Hardin J (2005) Diurnal cycle of tropical precipitation in Tropical Rainfall Measuring Mission (TRMM) satellite and ocean buoy rain gauge data. J Geophys Res 110:D21104

Brito SSB, Oyama MD (2014) Daily cycle of precipitation over the northern coast of Brazil. J Appl Meteorol Climatol 53:2481–2502

Cohen JCP, Dias AFSM, Nobre CA (1995) Environmental conditions associated with Amazonian squall lines: a case study. Mon Weather Rev 123:3163–3174

Cutrim EMC, Martin DW, Butzow DG, Silva IM, Yulaeva E (2000) Pilot analysis of hourly rainfall in central and eastern Amazonia. J Clim 13:1326–1334

da Rocha RP, Morales CA, Cuadra SV, Ambrizzi T (2009) Precipitation diurnal cycle and summer climatology assessment over South America: an evaluation of Regional Climate Model version 3 simulations. J Geophys Res 114: D10108

Dai A (2006) Precipitation characteristics in eighteen coupled climate models. J Clim 19:4605–4630

Dai A, Giorgi F, Trenberth KE (1999) Observed and model-simulated diurnal cycle of precipitation over the contiguous United States. J Geophys Res 104:6377–6402

Dai A, Xin L, Hsu KL (2007) The frequency, intensity, and diurnal cycle of precipitation in surface and satellite observations over low- and mid-latitudes. Clim Dyn 29:727–744

Demaria EMC, Rodriguez DA, Ebert EE, Salio P, Su F, Valdes JB (2011) Evaluation of mesoscale convective systems in South America using multiple satellite products and object-based approach. J Geophys Res 116: D08103

Dickinson RE, Henderson-Sellers A, Kennedy PJ (1993) Biosphere–Atmosphere Transfer Scheme (BATS) version 1E as coupled to the NCAR community climate model. Tech Note NCAR/TN-3871STR. National Center for Atmospheric Research, Boulder, CO

Dirmeyer PA, Cash BA, Kinter JL III, Jung T and others (2012) Simulating the diurnal cycle of rainfall in global climate models: resolution versus parameterization. Clim Dyn 39:399–418

Durkee J, Mote TL (2010) A climatology of warm-season mesoscale convective complexes in subtropical South America. Int J Climatol 30:418–431

Ferreira DBS, de Souza EB, de Moraes BC (2014) Ciclo horário da precipitação no leste da Amazônia durante o período chuvoso. Rev Bras Climatol 13:74–86

Freitas ED, Rozoff CM, Cotton WR, Dias PLS (2007) Interactions of an urban heat island and sea-breeze circulations during winter over the metropolitan area of São Paulo, Brazil. Boundary-Layer Meteorol 122:43–65

Garreaud R, Falvey M (2009) The coastal winds off western subtropical South America in future climate scenarios. Int J Climatol 29:543–554

Garreaud RD, Wallace JM (1997) The diurnal march of convective cloudiness over the Americas. Mon Weather Rev 125:3157–3171

Garstang M, Massie HL, Halverson J, Greco S, Scala J (1994) Amazon coastal squall lines. I. Structure and kinematics. Mon Weather Rev 122:608–622

Giorgi F, Coppola E, Solmon F, Mariotti L and others (2012) RegCM4: model description and preliminary tests over multiple CORDEX domains. Clim Res 52:7–29

Giorgi F (2014) Introduction to the special issue: the phase I CORDEX RegCM4 hyper-matrix (CREMA) experiment. Clim Change 125:1–5

Holtslag A, de Bruijn E, Pan HL (1990) A high resolution air mass transformation model for short-range weather forecasting. Mon Weather Rev 118:1561–1575

Hoskins BJ, Hodges KI (2005) A new perspective on Southern Hemisphere storm tracks. J Clim 18:4108–4129

Huffman GJ, Bolvin DT, Nelkin EJ, Wolff DB and others (2007) The TRMM Multisatellite Precipitation Analysis (TMPA): quasi-global, multiyear, combined-sensor precipitation estimates at fine scales. J Hydrometeorol 8: 38–55

Imaoka K, Spencer RW (2000) Diurnal variation of precipitation over the tropical oceans observed by TRMM/TMI combined with SSM/I. J Clim 13:4149–4158

Janowiak JE, Kousky VE, Joyce RJ (2005) Diurnal cycle of precipitation determined from the CMORPH high spatial and temporal resolution global precipitation analyses. J Geophys Res 110:D23105

Kanamitsu M, Ebisuzaki W, Woollen J, Yang SK, Hnilo JJ, Fiorino M, Potter G (2002) LNCEP-DOE AMIP-II Reanalysis (R2). Bull Am Meteorol Soc 83:1631–1643

Kikuchi K, Wang B (2008) Diurnal precipitation regimes in the global tropics. J Clim 21:2680–2696

Kousky VE (1980) Diurnal rainfall variation in northeast Brazil. Mon Weather Rev 108:488–498

Kubota T, Shige S, Hashizume H, Aonashi K and others (2007) Global precipitation map using satellite-borne

microwave radiometers by the GSMaP project: production and validation. IEEE Trans Geosci Remote Sens 45: 2259–2275

Laing AG, Fritsch JM (1997) The global population of mesoscale convective complexes. QJR Meteorol Soc 123: 389–405

Liang XZ, Li L, Dai A, Kunkel KE (2004) Regional climate model simulation of summer precipitation diurnal cycle over the United States. Geophys Res Lett 31:L24208

Lin XL, Randall DA, Fowler LD (2000) Diurnal variability of the hydrologic cycle and radiative fluxes: comparisons between observations and a GCM. J Clim 13:4159–4179

Llopart M, Coppola E, Giorgi F, da Rocha RP, Cuadra SV (2014) Climate change impact on precipitation for the Amazon and La Plata basins. Clim Change 125:111–125

Ma HY, Mechoso R (2007) Submonthly variability in the South American monsoon system. J Meteorol Soc Jpn 85: 381–401

Mapes BE, Warner TT, Xu MU (2003) Diurnal patterns of rainfall in northwestern South America. III. Diurnal gravity waves and nocturnal convection offshore. Mon Weather Rev 131:830–844

Marengo JA, Liebmann B, Grimm AM, Misra V and others (2012) Recent developments on the South American monsoon system. Int J Climatol 32:1–21

Martin GM, Bellouin N, Collins WJ, Culverwell ID and others (2011) The HadGEM2 family of Met Office Unified Model climate configurations. Geosci Model Dev 4:765–841

Meehl GA, Bony S (2011) Introduction to CMIP5. CLIVAR Exchanges 56:4–5

Mohr KI, Zipser EJ (1996) Mesoscale convective systems defined by their 85 GHz ice scattering signature: size and intensity comparison over tropical oceans and continents. Mon Weather Rev 124:2417–2437

Mota GV (2003) Characteristics of rainfall and precipitation features defined by the tropical rainfall measuring mission over South America. PhD dissertation, The University of Utah, Salt Lake City, UT

Mourão C, Chou SC, Marengo J (2016) Downscaling climate projections over La Plata Basin. Atmos Clim Sci 6:1–12

Pal JS, Giorgi F, Bi X, Elguindi N and others (2007) Regional climate modeling for the developing world: the ICTP RegCM3 and RegCNET. Bull Am Meteorol Soc 88: 1395–1409

Pereira Filho A, Carbone R, Tuttle J (2014) Convective rainfall systems in the La Plata Basin. Atmos Clim Sci 4:757–778

Pereira Filho A, Carbone R, Tuttle J, Karam H (2015) Convective rainfall in Amazonia and adjacent tropics. Atmos Clim Sci 5:137–161

Prakash S, Mitra AK, Rajagopal EN, Pai DS (2016) Assessment of TRMM-based TMPA-3B42 and GSMaP precipitation products over India for the peak southwest monsoon season. Int J Climatol 36:1614–1631

Randall DA, Harshvardan, Dazlich DA (1991) Diurnal variability of the hydrologic cycle in a general circulation model. J Atmos Sci 48:40–62

Reboita MS, Ambrizzi T, da Rocha RP (2009) Relationship between the Southern Annular Mode and Southern Hemisphere Atmospheric Systems. Rev Bras Meteorol 24:48–55

Reboita MS, Gan MA, da Rocha RP, Ambrizzi T (2010a) Regimes de precipitação na América do Sul: uma revisão bibliográfica. Rev Bras Meteorol 25:185–204

Reboita MS, da Rocha RP, Ambrizzi T, Sugahara S (2010b) South Atlantic Ocean cyclogenesis climatology simulated by regional climate model (RegCM3). Clim Dyn 35: 1331–1347

Reboita MS, da Rocha RP, Ambrizzi T (2012) Dynamic and climatological features of cyclonic developments over southwestern South Atlantic Ocean. In: Veress B, Szigethy J (eds) Horizons in earth science research, Vol 6. Nova Science Publishers, Hauppauge, NY, p 135–160

Reboita MS, da Rocha RP, Dias CG, Ynoue RY (2014) Climate projections for South America: RegCM3 driven by HadCM3 and ECHAM5. Adv Met 2014:1–17

Riahi K, Rao S, Krey V, Cho C and others (2011) RCP 8.5 — a scenario of comparatively high greenhouse gas emissions. Clim Change 109:33–57

Salio PM, Nicolini M, Zipser EJ (2007) Mesoscale convective systems over southeastern South American. Mon Weather Rev 135:1290–1309

Santos Silva CM (2013) Ciclo diário e semidiário de precipitação na costa norte do Brasil. Rev Bras Meteorol 28: 34–42

Satyamurty P, Mattos LF (1989) Climatological lower tropospheric frontogenesis in the midlatitudes due to horizontal deformation and divergence. Mon Weather Rev 117: 1355–1364

Saulo C, Ruiz J, Skabar YG (2007) Synergism between the low-level jet and organized convection at its exit region. Mon Weather Rev 135:1310–1326

Silva Dias PL, Bonatti JP, Kousky VE (1987) Diurnal forced tropical tropospheric circulation over South America. Mon Weather Rev 115:1465–1478

Solman S, Sanchez E, Samuelsson P, da Rocha RP and others (2013) Evaluation of an ensemble of regional climate model simulations over South America driven by the ERA-Interim reanalysis: model performance and uncertainties. Clim Dyn 41:1139–1157

Teixeira RFB (2008) O fenômeno da brisa e sua relação com a chuva sobre Fortaleza-CE (The breeze phenomenon and its relationship with the rain over Fortaleza-CE). Rev Bras Meteorol 23:282–291 (in Portuguese with English abstract)

Velasco I, Fritsch JM (1987) Mesoscale convective complexes in the Americas. J Geophys Res 92:9591–9613

Vera C, Higgins W, Ambrizzi T, Amador J and others (2006) Toward a unified view of the American monsoon systems. J Clim 19:4977–5000

Warner TT, Mapes BE, Xu M (2003) Diurnal patterns of rainfall in northwestern South America. II. Model simulations. Mon Weather Rev 131:813–829

Xie P, Arkin PA (1997) Global precipitation: a 17-year monthly analysis based on gauge observations, satellite estimates, and numerical model outputs. Bull Am Meteorol Soc 78:2539–2558

Yang GY, Slingo J (2001) The diurnal cycle in the Tropics. Mon Weather Rev 129:784–801

Editorial responsibility: Filippo Giorgi, Trieste, Italy

Submitted: April 18, 2016; Accepted: July 20, 2016
Proofs received from author(s): August 30, 2016